Electron diffraction using ultrafast electron bunches from a laser-wakefield accelerator at kHz repetition rate

Z.-H He, A. G. R. Thomas, B Beaurepaire, J. A. Nees, B Hou, Victor Malka, K Krushelnick, Jérôme Faure

Electron diffraction using ultrafast electron bunches from a laser-wakefield accelerator at kHz repetition rate

Z.-H. He[1], A. G. R. Thomas[1], B. Beaurepaire[2], J. A.

Nees[1], B. Hou[1], V. Malka[2], K. Krushelnick[1], and J. Faure[2]

[1]*Center for Ultrafast Optical Science, University of Michigan,*

Ann Arbor, MI 48106-2099 USA and

[2]*Laboratoire d'Optique Appliquée, ENSTA-CNRS-Ecole Polytechnique,*

UMR 7639, 91761 Palaiseau, France

(Dated: January 29, 2013)

Abstract

We show that electron bunches in the 50-100 keV range can be produced from a laser wakefield accelerator using 10 mJ, 35 fs laser pulses operating at 0.5 kHz. It is shown that using a solenoid magnetic lens, the electron bunch distribution can be shaped. The resulting transverse and longitudinal coherence is suitable for producing diffraction images from a polycrystalline 10 nm aluminum foil. The high repetition rate, the stability of the electron source and the fact that its uncorrelated bunch duration is below 100 fs make this approach promising for the development of sub-100 fs ultrafast electron diffraction experiments.

Ultrafast electron diffraction (UED) is a powerful technique for investigating structural dynamics in matter [1, 2]. For example, the dynamics of the melting transition have been elucidated on the sub-500 fs time scale in metals [3] or semi-metals [4]; structural phase transitions have also been studied in more complex materials, such as VO_2 [5] or the charge density wave material $1T - TaS_2$ [6]. The state of the art of electron sources for ultrafast electron diffraction consists of electron bunches generated from photocathodes and subsequently accelerated in static fields, providing $\simeq 50 - 100$ keV kinetic energy. The shortest electron bunches produced in this way are in the 300-500 fs range, with thousands of electrons per bunch [2]. These limitations are essentially due to two factors: (i) the space charge of the beam which limits the number of electrons and the temporal resolution, and (ii) the ballistic propagation of electrons with various velocities, which produces a linear chirp (i.e. a longitudinal momentum-position correlation in the phase space) and also tends to degrade the temporal resolution. The second issue has recently been solved by using a Radio-Frequency (RF) cavity in order to change the sign of the chirp and compress the electron bunch down to 80 fs [7, 8]. Concerning the first issue, current developments tend to promote the use of RF guns in order to accelerate electrons to MeV energies in higher electric fields for mitigating the effect of space charge [9–12]. In addition to larger accelerating gradients, the RF fields can also be used to compress the electron bunches and very short bunch durations are predicted [13]. However, it should be noted that the use of RF technology tends to introduce jitter in pump-probe experiments and can thus limit the temporal resolution, in particular when accumulation over several shots is required [14]. At this point, no UED experiment with a resolution lower than 100 fs has been achieved even though in principle sub-100 fs electron bunches have been demonstrated.

Another approach consists of using electrons produced in high intensity laser-plasma interaction experiments. In such interactions, plasma electrons are accelerated by laser and/or plasma fields and can gain MeV energies in micron distances, thus mitigating the effect of space charge. At the source, there is no chirp and in consequence, the electron bunch duration can be shorter than the laser pulse duration. In addition, the electron bunch is produced directly by the laser pulse in a jitter free manner which therefore reduces the temporal resolution in pump-probe experiments. However, electron bunches from laser-plasma interaction have relatively large energy spreads: bunches produced from laser-solid interaction typically have $\delta E/E$ of tens of percent [15] whereas bunches from underdense plasmas

2

can have $\delta E/E$ of a few percent [16–18]. Consequently, the electron bunch develops a linear chirp as it propagates which can severely degrade the bunch duration for sub-relativistic or moderately relativistic beams as used in UED experiments. For UED applications, electron bunches from plasmas should be manipulated and the linear chirp can be compensated using existing magnetic optics technology [19]. Tokita et al. [20] have recently performed high-intensity laser-solid interaction experiment and demonstrated that electrons originating from the back of a solid target can be used to obtain single shot and high quality diffraction images. A temporal resolution of 500 fs was obtained after compensation of the linear chirp [21] so that the temporal resolution might be due to the intrinsic bunch duration given by the interaction mechanism: electron recirculation in the target might elongate the bunch duration.

In contrast, electrons generated from a laser wakefield accelerator [22] can intrinsically provide shorter bunch durations in the 1-10 fs range [23]. Such short durations can be explained by the acceleration mechanism: electrons are injected in a plasma wave bucket the length of which is given by the plasma wavelength λ_p. The electron bunch occupies a small fraction of the bucket, and has a duration typically $< \lambda_p/2c$, e.g. < 15 fs for an electron density of $n_e = 10^{19}\,\mathrm{cm}^{-3}$. Relativistic electron bunches in the 100 MeV - 1 GeV range are produced with Joule level laser systems operating at 10 Hz or below. Their energy is too high for practical applications in UED. However, the scalability of laser wakefield accelerators has been recently demonstrated [24] and can be extended to a few mJ kHz laser system for producing electrons [25, 26]. This electron source has strong potential for UED experiments: (i) after removing the linear chirp, the bunches should be sub-100 fs, (ii) electron bunches are intrinsically synchronized to the laser source, (iii) the gas target and the high repetition rate permit an ease of use as well as the possibility to accumulate data.

Before moving on to time resolved studies, it is important to show that electron bunches from a laser wakefield accelerator have sufficient quality for producing a diffraction pattern. In this letter, we use a laser wakefield accelerator operating at high repetition rate (0.5 kHz) in order to produce 50-100 keV electrons. By focusing the electron beam using a solenoid, we show that the transverse and energy distributions of the beam can be manipulated. The resulting beam quality is sufficient to provide diffraction images from a polycrystalline Al sample.

The experimental set-up is shown on Figure 1. A Ti:Sapphire laser system operating at

(a)

laser

pinhole   solenoid   spectrometer   FOS

CCD

capillary
gas jet   lens
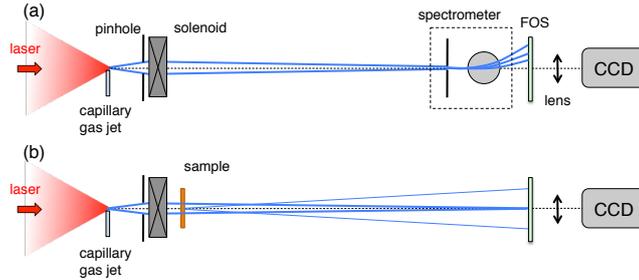
(b)

sample

laser

CCD

capillary
gas jet

FIG. 1: (a) Experimental set-up for electron beam characterization with an electron spectrometer. (b) Set-up for diffraction. The solenoid is placed 60 mm after the electron source, the distance between the sample and the scintillator (FOS) is 220 mm.

0.5 kHz delivers 7.4 mJ pulses on target at wavelength $\lambda_0 = 800$ nm in a 35 fs duration at Full Width Half Maximum (FWHM). The laser pulses are focused down to 2.5 microns (FWHM) using an $f\# = 2$ off-axis parabola. The beam is focused into free flowing argon gas at $300\,\mu$m above a $100\,\mu$m diameter capillary gas jet. The electron density after ionization by the laser pulse is estimated using interferometry to be $\simeq 10^{19}\,\text{cm}^{-3}$. The residual pressure in the vacuum chamber stays below 10^{-3} mbar which permits the operation of the electron source at 0.5 kHz. The electrons produced in the interaction are first filtered by a 1 mm pinhole before they travel through a solenoid magnetic lens. The electron beam profile is measured on a CsI(Tl) scintillator plate deposited on top of a fiber optic plate (J6677 FOS by Hamamatsu), which is imaged on a CCD camera. The electron beam energy distribution is obtained by inserting a removable electron spectrometer comprising a 20 mm dipole magnet (providing a 25 mT magnetic field) and a $500\,\mu$m wide aluminum slit. The FOS response to electrons has been carefully calibrated using an electron microscope in the range 50-300 keV. The detector has a very small response below 50 keV so that in practice, electrons below 50 keV are not detected. We use this calibrated response to obtain the absolute number of electrons per shot and to deconvolve the raw electron distribution. This point is important because the response of scintillators is far from flat when the electron energy is comparable to the energy deposited in the material [27, 28].

Figure 2(a) shows the beam profile onto the scintillator after filtering by the pinhole whereas fig. 2(b) shows the beam profile when the electron beam is focused on the scintillator using the magnetic lens. Fig. 2(c) shows the profile of the electron beam at focus (red curve);

it is well fitted by a Lorentzian function with a FWHM of $D = 280\,\mu$m. The Lorentzian shape comes from the fact that the beam is polychromatic: the lower energies form a halo around the focused beam.
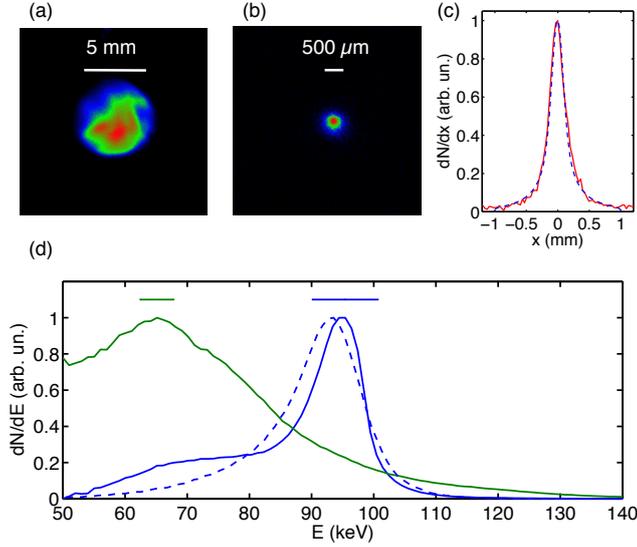

FIG. 2: (a) Unfocused beam after filtering through a 1 mm pinhole. (b) Best focus obtained using the solenoid. The FWHM is $D = 280\,\mu$m. (c) Horizontal lineout of the beam profile (red curve) and GPT simulation results (blue curve). (d) Normalized electron distribution of the unfocused beam (green curve), focused beam (blue curve) and simulation results of the focused beam (dashed blue curve). The top error bars represent the resolution of the spectrometer at various energies.

The energy distributions measured using the magnetic spectrometer are shown in fig. 2(d). When the beam is unfocused (green curve), the energy distribution is wide with a cut-off at 50 keV corresponding to the scintillator cut-off. The blue curve shows the spectrum obtained by integrating over the focal point when the solenoid is used. The chromaticity of the magnetic lens permits some shaping of the energy distribution: the distribution peaks at 95 keV and has a FWHM $\delta E/E = 7.5\%$. Using the calibrated scintillator, we found that the beam charge is up to 8×10^4 electrons/bunch (12 fC/bunch), with 14% RMS fluctuations, which fall down to 7.9% when the images are averaged over 10 shots. When the beam is focused, the number of electrons per bunch in the focus (integrated around 2σ RMS) is 3×10^4, i.e. 4.5 fC/bunch. The energy distribution is extremely stable and its shape does not fluctuate significantly. Finally, the pointing stability of the focused beam is found to be

greater than the angular resolution of the imaging system, i.e. $400\,\mu\mathrm{rad}$. The stability of the electron beam is found to be superior to those reported in the literature on laser wakefield acceleration [16, 17]. This might be due to the fact that a kHz laser system is usually more compact and stable than a multi-joule laser system. In addition, the injection mechanism that is used in this experiment relies on downramp injection [26, 29] and it does not rely on the non linear evolution of the laser pulse which tends to be detrimental for obtaining a stable electron beam. This high level of stability will be of crucial importance for UED experiments where the intensity and position of Bragg peaks need to be monitored with high accuracy.

The bunch propagation in the beam line was modeled using the GPT (General Particle Tracer) code. We found that the experimental beam profile could be reproduced by using an initial transverse gaussian distribution with a rms radius of $15\,\mu\mathrm{m}$: the result is shown as the blue curve in fig. 2(c). In addition, the calculated energy distribution in the focused beam agrees well with the experiment (dashed blue curve in fig. 2(d). From the GPT calculation, it was possible to retrieve upper values of the normalized emittance in the focused beam (integrated around 2σ RMS): $\varepsilon_N = 2 \times 10^{-2}$ mm.mrad. The transverse coherence is then given by $L = \hbar D/mc\varepsilon_N \simeq 5$ nm, a value suitable for performing electron diffraction.
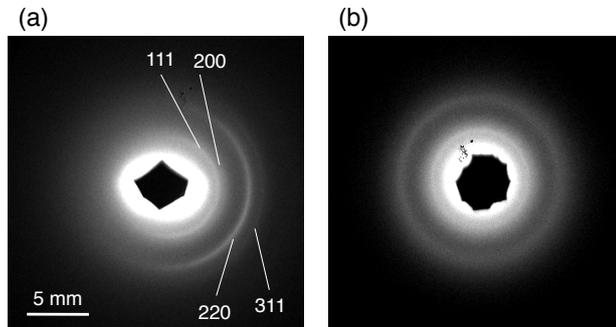

FIG. 3: Electron diffraction patterns from a 10 nm thick polycrystalline Al foil. (a) The diffraction pattern is assymetric because of a spatial chirp in the electron beam. (b) Symmetric diffraction pattern obtained by removing the spatial chirp on the electron beam.

The diffraction patterns were obtained using a 10 nm thick polycrystalline aluminum sample. The Al foil was free standing on an mesh as used in transmission electron microscopy. In fig. 3(a), one can clearly see the rings from the (111) and (220) planes; the rings originating

from diffraction on the (200) and (311) planes are also visible although dimmer. Note that this image displays an asymmetric ring pattern. This is due to the fact that the solenoid was not perfectly aligned on the electron beam axis. In consequence, because the electron beam has a large energy distribution, a spatial chirp is present at focus. Such a spatial chirp can cause an asymmetric modification of the diffraction pattern as observed in Ref. [30]. We found that the solenoid alignment is extremely sensitive, in particular because the electron beam has such a large energy distribution. When the solenoid is well aligned, the beam focal spot is symmetric, indicating that no spatial chirp is present and the diffraction pattern is symmetric, fig. 3(b). Note that in that image, the diffraction rings are broader. This is because for this particular data set, the energy distribution of the electron beam was broader than for image a). Nevertheless, the clear diffraction pattern shows that despite a large energy spread, these electron bunches have sufficient transverse and longitudinal coherence. In fig. 3 both images were obtained by accumulating data over tens of seconds. Diffraction rings could be clearly measured by accumulating 200 shots or more. In Ref. [20], single shot diffraction patterns have been recorded from a single crystal. As our electron source provides a similar number of electrons/shot, we believe that extension to single shot data could be performed by (i) using a single crystal sample (ii) increasing the effective quantum efficiency (QE) of our detection system. We estimate the current effective QE (i.e. photons emitted by the FOS to counts) of our detection system to be $\simeq 8 \times 10^{-5}$, a value which could be increased by more than one order of magnitude by using a more sensitive camera and increasing the collection angle of our imaging system.

In conclusion, we have developed a laser wakefield accelerator operating at 0.5 kHz and producing stable electron bunches at about 100 keV. By manipulating the beam with a solenoid, we have been able to increase the beam quality and to produce diffraction patterns from a polycrystalline Al sample. This first proof-of-principle experiment shows the potential of high repetition rate, low energy electron bunches from laser wakefield accelerators for applications in ultrafast electron diffraction.

and DARPA under Contract No. N66001-11-1-4208.

[1] A. H. Zewail and J. M. Thomas, *4D electron microscopy* (Imperial College Press, London, 2009).

[2] G. Sciaini and R. J. D. Miller, Rep. Prog. Phys. **74**, 096101 (2011).

[3] B. J. Siwick, J. R. Dwyer, R. E. Jordan, and R. J. D. Miller, Science **302**, 1382 (2003).

[4] G. Sciaini, M. Harb, S. G. Kruglik, T. Payer, C. T. Hebeisen, F. M. zu Heringdorf, M. Yamagushi, M. H. von Hoegen, R. Ernstorfer, and R. J. D. Miller, Nature **458**, 458 (2009).

[5] P. Baum, D.-S. Yang, and A. Zewail, Science **318**, 788 (2007).

[6] M. Eichberger, H. Schäfer, M. Krumova, M. Beyer, J. Demsar, H. B. abd G. Moriena, G. Sciani, and R. J. D. Miller, Nature **468**, 799 (2010).

[7] T. van Oudheusden, E. F. de Jong, S. B. van der Geer, W. P. E. M. Op't Root, O. J. Luiten, and B. J. Siwick, J. Appl. Phys. **102**, 093501 (2007).

[8] T. van Oudheusden, P. L. E. M. Pasmans, S. B. van der Geer, M. J. de Loos, M. J. van der Wiel, and O. J. Luiten, Phys. Rev. Lett. **105**, 264801 (2010).

[9] J. B. Hastings, F. M. Rudakov, D. H. Dowell, J. F. Schmerge, J. D. Cardoza, J. M. Castro, S. M. Gierman, H. Loos, and P. M. Weber, Appl. Phys. Lett. **89**, 184109(2006).

[10] P. Musumeci, J. T. Moody, C. M. Scoby, M. S. Gutierrez, H. A. Bender, and N. S. Wilcox, Rev. Sci. Instrum. **81**, 013306 (2010).

[11] R. Li, W. Huang, Y. Du, L. Yan, Q. Du, J. Shi, J. Hua, H. Chen, T. Du, H. Xu, *et al.*, Rev. Sci. Instrum. **81**, 036110 (2010).

[12] Y. Murooka, N. Naruse, S. Sakakihara, M. Ishimaru, J. Yang, and K. Tanimura, Appl. Phys. Lett. **98**, 251903 (2011).

[13] J.-H. Han, Phys. Rev. ST Accel. Beams **14**, 050101 (2011).

[14] P. Musumeci, J. T. Moody, C. M. Scoby, M. S. Gutierrez, and M. Westfall, Appl. Phys. Lett. **97**, 063502 (2010).

[15] A. G. Mordovanakis, J. Easter, N. Naumova, K. Popov, P.-E. Masson-Laborde, B. Hou, I. Sokolov, G. Mourou, I. V. Glazyrin, W. Rozmus, *et al.*, Phys. Rev. Lett. **103**, 235001 (2009).

[16] W. P. Leemans, B. Nagler, A. J. Gonsalves, C. Tòth, K. Nakamura, C. G. R. Geddes, E. Esarey,

C. B. Schroeder, and S. M. Hooker, Nat. Phys. **2**, 696 (2006).

[17] J. Faure, C. Rechatin, A. Norlin, A. Lifschitz, Y. Glinec, and V. Malka, Nature **444**, 737 (2006).

[18] C. Rechatin, J. Faure, A. Ben-Ismail, J. Lim, R. Fitour, A. Specka, H. Videau, A. Tafzi, F. Burgy, and V. Malka, Phys. Rev. Lett. **102**, 164801 (2009).

[19] P. Kung, H.-C. Lihn, and H. Wiedmann, Phys. Rev. Lett. **73**, 967 (1994).

[20] S. Tokita, S. Inoue, S. Masuno, M. Hashida, and S. Sakabe, Appl. Phys. Lett. **95**, 111911 (2009).

[21] S. Tokita, M. Hashida, S. Inoue, T. Nishoji, K. Otani, and S. Sakabe, Phys. Rev. Lett. **105**, 215004 (2010).

[22] E. Esarey, C. B. Schroeder, and W. P. Leemans, Rev. Mod. Phys. **81**, 1229 (2009).

[23] O. Lundh, J. Lim, C. Rechatin, L. Ammoura, A. Ben-Ismail, X. Davoine, G. Gallot, J.-P. Goddet, E. Lefebvre, V. Malka, and J. Faure, Nat. Phys. **7**, 219 (2011).

[24] K. Schmid, L. Veisz, F. Tavella, S. Benavides, R. Tautz, D. Herrmann, A. Buck, B. Hidding, A. Marcinkevicius, U. Schramm, *et al.*, Phys. Rev. Lett. **102**, 124801 (2009).

[25] A. F. Lifschitz and V. Malka, New J. Phys. **14**, 053045 (2012).

[26] Z.-H. He, B. Hou, J. H. Easter, K. Krushelnick, J. A. Nees, and A. G. R. Thomas, submitted to New J. Phys. (2013).

[27] K. A. Tanaka, T. Yabuuchi, T. Sato, R. Kodama, Y. Kitagawa, T. Takahashi, T. Ikeda, Y. Honda, and S. Okuda, Rev. Sci. Instrum. **76**, 013507 (2005).

[28] Y. Glinec, J. Faure, A. Guemnie-Tafo, V. M. H. Monard, J. P. Larbre, V. D. Waele, J. L. Marignier, and M. Mostafavi, Rev. Sci. Instrum. **77**, 103301 (2006).

[29] S. Bulanov, N. Naumova, F. Pegoraro, and J. Sakai, Phys. Rev. E **58**, R5257 (1998).

[30] E. E. Fill, S. Trushin, R. Bruch, and R. Tommasini, Appl. Phys. B **81**, 155 (2005), ISSN 0946-2171.